



Planetary Rings Workshop

Program

August 13 - 15, 2014
CU-LASP, Boulder, Colorado
Larry Esposito, Host

PLANETARY RINGS WORKSHOP

August 13-15, 2014
CU-LASP, 3665, Discovery Drive, Boulder, Colorado
SPSC Building, Room W120
Hosted by Larry Esposito

Welcome

This workshop is open to all interested parties, and any observational or theoretical research on the properties, dynamics, origin or evolution of any planetary ring system is appropriate. This meeting will highlight the latest Cassini results. We will have all oral talks; 15 minutes for each presentation with 10 minutes for questions. Ample time will be allowed for discussion. Previous workshops were held in Ithaca (2011), Paris (2008) and Whitefish, MT (2006). The scientific organizing committee was composed of Larry Esposito, Glen Stewart, Shawn Brooks and Jeff Cuzzi.— *Larry Esposito and Laura Bloom*

Table of Contents

| | |
|---|----|
| WELCOME..... | 1 |
| SCHEDULE..... | 2 |
| ABSTRACTS..... | 5 |
| WEDNESDAY AUGUST 13 | 5 |
| <i>Opening Session</i> | 5 |
| <i>Macro Structure</i> | 5 |
| <i>Clumps and Clusters</i> | 8 |
| <i>Microstructure and Composition</i> | 10 |
| THURSDAY, AUGUST 14 | 12 |
| <i>Microstructure and Composition—Continued</i> | 12 |
| <i>Photometry</i> | 13 |
| <i>Dynamics and Kinematics</i> | 14 |
| FRIDAY, AUGUST 15 | 19 |
| <i>F Ring</i> | 19 |
| <i>Origin, evolution</i> | 20 |
| <i>Ring environment</i> | 23 |
| RECEPTION..... | 25 |
| DINNER..... | 25 |
| GETTING AROUND | 26 |

Schedule

—All oral talks are 15 minutes with 10 minutes for discussion—

Tuesday August 12

Reception

5:30-7:30

Millennium Harvest House

Wednesday August 13

8:30AM

Opening session

Welcome

Housekeeping

Announcement—Icarus special issue

Announcement—Ring conference

*Ten years at Saturn and more surprises
on the way*

Larry W. Esposito

Laura Bloom

Phil Nicholson

Matthew S. Tiscereno

Linda Spilker

Macrostructure, Chair: Joshua E. Colwell

A new moon-induced structure

*Towards an understanding of thermal
throughput across Saturn's rings
with Cassini CIRS*

Nicole Albers

Shawn M. Brooks

Break

10:15 – 10:30

Load presentations

Thermal studies of the B-Ring

A few new things in Saturn's D ring

Stuart Pilorz

Matthew M. Hedman

Group Photo

11:20 – 11:30

Gather out front

Lunch

11:30 – 1:00pm

On your own

Clumps and clusters, Chair: Glen R. Stewart

*Studying sizes and shapes of particle
agglomerates from occultation statistics*

Predator-prey model for A-Ring haloes

*Particle & particle-cluster sizes in
Saturn's rings from Cassini radio
occultations*

Joshua E. Colwell

Larry W. Esposito

Essam Marouf

*Searching for clumps in Main Ring
spiral density waves*

Morgan E. Rehnberg

Break

2:40 – 2:55

Load presentations

Propellers in Saturn's rings

*Orbit evolution of disk-embedded masses:
Directly observed in Saturn's rings*

Miodrag Sremcevic

Matthew S. Tiscereno

Microstructure and Composition, Chair: Linda Spilker

| | |
|--|-----------------|
| <i>Comparison of Cassini UVIS reflectance spectra of Saturn's rings to compositional models</i> | Eric T. Bradley |
| <i>Study of Saturn's rings based on analysis of dust impact signals captured by Cassini RPWS</i> | Sheng-Yi Ye |
| <i>Observing Saturn's rings in the microwave with Cassini</i> | Zhimeng Zhang |

Adjourn 5:00

Dinner 6:30 [Cantina Loredò](#)

Thursday August 14

9:00AM

Microstructure and Composition, Chair: Linda Spilker—*Continued*

| | |
|--|--------------|
| <i>Constraining the micro and macro-structure of the Saturn's rings by modeling optical and thermal opposition phase curves of Cassini</i> | Estelle Deau |
|--|--------------|

| | |
|--|-----------------|
| <i>Incomplete cooling of Saturn's A ring at equinox: Implication for seasonal thermal inertia and internal structure of ring particles</i> | Ryuji Morishima |
|--|-----------------|

Photometry, Chair: Shawn M. Brooks

| | |
|---|-----------------|
| <i>Measuring sub-centimeter particles in Saturn's A ring with Cassini UVIS stellar occultations</i> | Tracy M. Becker |
|---|-----------------|

Break 10:15 – 10:30 [Load presentations](#)
Rebecca Harbison

| | |
|--|---------------------|
| <i>Stellar occultation measurements of particles in Saturn's rings</i> | Richard G. Jerousek |
| <i>Small particle population in Saturn's rings from self-gravity wake observations</i> | |

Lunch 11:30 – 1:00pm [On your own](#)

Dynamics and Kinematics, Chair: Matthew S. Tiscereno

| | |
|--|-------------------|
| <i>Deciphering the embedded wave in Saturn's Maxwell Ringlet</i> | Richard G. French |
|--|-------------------|

| | |
|---|-------------|
| <i>Collisions between gravitational aggregates in the tidal field</i> | Ryuki Hyodo |
|---|-------------|

| | |
|---|-----------------------|
| <i>A prominent $m=1$ standing wave in the Cassini Division</i> | Colleen McGhee-French |
|---|-----------------------|

| | |
|--|----------------|
| <i>Kronoseismology II: Further searches for Saturn-driven waves in the C ring.</i> | Phil Nicholson |
|--|----------------|

Break 2:40 – 2:55 [Load presentations](#)

| | |
|--|-------------------|
| <i>Particle clustering in periodically forced planetary rings</i> | Stuart J. Robbins |
| <i>Gravitational accretion of particles onto moonlets embedded in Saturn's Rings</i> | Yuki Yasui |
| <i>On the origin of eccentric narrow rings</i> | Glen R. Stewart |
| <i>The stable F Ring core: Antiresonance plus corotation resonance</i> | Jeff Cuzzi |
| <i>Adjourn</i> | 5:00 |

Friday August 15

9:00AM

| | |
|---|--------------------------|
| F Ring , Chair: Jeff Cuzzi | |
| <i>Gravitational and collisional processes at Saturn's F Ring</i> | Mike Evans (C.D. Murray) |
| <i>Comparison of clumps in Saturn's F Ring from Voyager and Cassini</i> | Robert S. French |
| <i>For there is nothing covered, that shall not be revealed: Unveiling Saturn's F ring at ring plane crossing</i> | Britt R. Scharringhausen |

Break

10:20 – 10:35

Load presentations

| | |
|--|-----------------------|
| Origin, evolution , Chair: Richard G. French | |
| <i>Recent results on Chariklo's rings</i> | Maryame El Moutamid |
| <i>Dynamics of Uranus' dusty μ ring</i> | Hsiang-Wen (Sean) Hsu |
| <i>Accretion of the Moon from the protolunar disk</i> | Julien Salmon |

Lunch

12:00 – 1:00pm

Catered on site

| | |
|--|--------------------|
| <i>Satellite formation from circumplanetary particle disks</i> | Ryuki Hyodo |
| <i>What happens to the Keeler gap when Daphnis decides to move out?</i> | Radwan Tajeddine |
| <i>Evolution of structure and composition in Saturn's Rings due to ballistic transport of micrometeoroid impact ejecta</i> | Paul R. Estrada |
| Ring environment , Chair: Matthew M. Hedman | |
| <i>The mass flux of micrometeoroids into the Saturnian system</i> | Sascha Kempf |
| <i>Saturn's other Ring current</i> | F. J. Crary |
| <i>OPUS: Now with enhanced geometric metadata for Cassini optical remote sensing instruments</i> | Mitchell K. Gordon |

Break

3:30 – 3:45

Load presentations

| | |
|---------------------------|----------------------------|
| <i>Wrap-up discussion</i> | Phil Nicholson (Moderator) |
| <i>Adjourn</i> | 5:00 |

Abstracts

Wednesday August 13

Opening Session

Ten Years at Saturn and more Surprises on the Way

Linda Spilker

Jet Propulsion Laboratory/California Institute of Technology, Pasadena, CA, USA, (Linda.J.Spilker@jpl.nasa.gov)

The Cassini-Huygens mission has greatly enhanced our understanding of the Saturn system. Fundamental discoveries have altered our views of Saturn, its retinue of icy moons including Titan, the dynamic rings, and the system's complex magnetosphere. Launched in 1997, the Cassini-Huygens spacecraft spent seven years traveling to Saturn, arriving in July 2004, roughly two years after the northern winter solstice. Cassini has orbited Saturn for 9.5 years, delivering the Huygens probe to its Titan landing in 2005, crossing northern equinox in August 2009, and completing its Prime and Equinox Missions. It is now three years into its 7-year Solstice mission, returning science in a previously unobserved seasonal phase between equinox and solstice. As it watches the approach of northern summer, long-dark regions throughout the system become sunlit, allowing Cassini's science instruments to probe as-yet unsolved mysteries.

Key Cassini-Huygens discoveries include icy jets of material streaming from tiny Enceladus' south pole, lakes of liquid hydrocarbons and methane rain on giant Titan, three-dimensional structures in Saturn's rings, and hurricanes at Saturn's poles. The Huygens probe sent back amazing images of Titan's surface, and made detailed measurements of the atmospheric composition, structure and winds. Key Cassini-Huygens science highlights will be presented.

Cassini-Huygens is a cooperative undertaking by NASA, the European Space Agency (ESA), and the Italian space agency (Agenzia Spaziale Italiana, ASI).

This work was carried out in part at the Jet Propulsion Laboratory, California Institute of Technology, under contract with NASA. Copyright 2014 California Institute of Technology. Government sponsorship is acknowledged.

Macro Structure

A new moon-induced structure

Nicole Albers

LASP, University of Colorado, Boulder, CO 80303, USA, (Nicole.Albers@lasp.colorado.edu)

Many structures in Saturn's rings result from gravitational perturbations of external and embedded moons. Among these are density waves, propeller structures, circumferential gaps, and kinematic wakes.

Cassini UVIS stellar occultations show gap-like features within a few tens of km of the Encke and Keeler gap edges. One of the inner Encke gap features was previously observed by the Voyager 2 PPS experiment. All are exclusively

found downstream of Pan and Daphnis, respectively. Their observed radial width measures few km across. Plotted versus relative azimuthal distance to the moon it exhibits a bell-shaped dependence. This supports the hypothesis that the individual features are multiple detections of a single, corotating density depletion. Special observation geometries of two occultations allow to further constrain its proportion.

Interestingly, none of these has been observed at the inner Keeler gap edge, where the temporal and spatial variability of the edge are still poorly understood and most likely driven by the Prometheus 32:31 ILR located nearby.

While the opening of a gap by and wakes of embedded objects are known since Voyager observations, these new results reveal the existence of a previously unknown and unpredicted moon-associated structure. Its existence offers another avenue in searching for embedded objects, although our preliminary search did not produce examples apart from those reported here for Pan and Daphnis.

We acknowledge Tracy Becker for providing an initial list of positive detections.

Towards an Understanding of Thermal Throughput across Saturn's Rings with Cassini CIRS

S. M. Brooks (1), L. J. Spilker (1), S. H. Piorz (2) and M. R. Showalter (2)

(1) Jet Propulsion Laboratory, California, USA (2) SETI Institute, Mountain View, California, USA

One of the more striking aspects of Saturn's main ring system is its aspect ratio. Although it spans over 270,000 km from ansa to ansa, its thickness normal to the ring plane is less than a million times its breadth. Hence, studies of the rings' structure focus mostly on radial and azimuthal features. And yet in the thermal infrared the finite vertical thickness of the main rings is clearly manifest as measured temperature differences between that face of the rings under direct solar illumination (the lit face) and the opposite (unlit) face derived from observations with Cassini's Composite Infrared Spectrometer (CIRS). The ultimate goal of this work is to understand these lit/unlit temperature differentials and their variation with radius and optical depth in order to infer information about the main rings' structure and dynamics in this third dimension.

As previous work has shown (Spilker *et al.*, 2006), the thermal flux from the rings observed by CIRS is a function of observing geometry. To control for these variations, we specifically designed paired observations of the lit and unlit sides rings where observing variables such as the emission, phase and local hour angles were as similar as possible to facilitate direct comparison between lit and unlit observations. This presentation is a progress report on our analysis of such observations and our plans for future work.

This research was carried out at the Jet Propulsion Laboratory, California Institute of Technology, under contract with NASA. Copyright 2014 California Institute of Technology. Government sponsorship acknowledged.

A few new things in Saturn's D ring

M. Hedman (#1), J. A. Burns, Z. Pontrantolfi, J.A. Burt, M.R. Showalter, P.D. Nicholson, M.S. Tiscareno.

The D ring is Saturn's innermost ring, and it is amongst the most dynamic and time-variable components of Saturn's ring system. Previous studies of this ring have shown significant changes in the ring's overall structure in the thirty years between when it was first observed by Voyager and when Cassini arrived at Saturn. Over the last decade, Cassini has observed steady changes in the morphology of multiple D-ring structures that provide clues about this region's dynamical environment and history. In particular, slowly evolving spiral patterns in the outer D ring suggest that some event disturbed Saturn's rings in 1983. Now, more thorough analyses of the Cassini data have revealed much more rapid changes in the D-ring's structure. For example, around 2009 one of the dusty ringlets in the outer D ring increased in brightness by almost a factor of three over the course of a year. More recently, a new spiral pattern appeared in the inner D ring, indicating that something disturbed the ring in late 2011, while Cassini was in orbit around Saturn. The potential causes and implications of these relatively rapid changes are currently under investigation.

Thermal Studies of the B-Ring

Pilorz, Stuart

We show results obtained from comparing the estimated net emitted flux from Saturn's B-ring with modeled incident flux during the Saturn season extending from Cassini's orbit insertion through Saturn equinox.

We estimate the net emitted flux noting that the thermal emission from the unlit B-Ring is nearly isotropic, while that from the lit ring is isotropic except for a "hot spot" around the zero-phase direction.

A detailed numerical integration is used to calculate the flux absorbed from the Sun and Saturn, and we find that the net emission balances the incident flux at all times and ring locations to within model and data accuracy.

The flux leaving the unlit B-Ring is approximately 30% of the flux incident on the lit side at all times and locations, and varies inversely with the lit emission across ring regions, suggesting that the unlit emission results from throughput energy. Detailed calculations show that the throughput varies linearly inversely with the normal optical depth.

A ramification of the observed high throughput is that the thermal conductivity of the ring must be higher than that of known icy regoliths. It is at the upper end of the range allowed by radiative-convective models for thermal transport being investigated by Ferrari and Reffet.

Coupled radiative-convective models require many parameters, and are subject to the curse of non-uniqueness when attempting to invert thermal data into ring and particle properties. We speculate on some leverage points for using such models.

Clumps and Clusters

Studying Sizes and Shapes of Particle Agglomerates from Occultation Statistics

Joshua E. Colwell (1), James H. Cooney (1), Larry W. Esposito(2)
University of Central Florida, (2) University of Colorado

The variance in the time series of star brightness in stellar occultations by the rings provides information on the autocorrelation function of the small-scale transparency distribution within the rings. In the simplest model of isolated, identical spherical particles, the transparency is zero where a ring particle is present, and where no particles are present the transparency is one. In this scenario the autocorrelation function is directly related to the size of the particles. The distribution of ring particles in Saturn's rings is in general more complicated than this, however. Non-axisymmetric elongated clumps of particles dominate the small-scale structure in the A and B rings, for example, and such structures will produce different variances depending on the observation geometry. We have found that the variance in different regions of the rings indicates different particle autocorrelation functions. Relating this directly to particle sizes, however, requires taking into account the full non-axisymmetric distribution of particle clumps. We present the results of Monte Carlo simulations of stellar occultations through various geometric models of ring particle distributions and discuss the relationship between occultation variance and ring particle sizes, shapes and orientations of clumps, distributions of particles in a monolayer or multi-layer system, and the effects of particle size distributions, including diffraction. We compare our results to UVIS stellar occultation observations.

Predator-Prey Model for A-Ring Halo

LW Esposito, P Madhusudhanan, M Sremcevic, JE Colwell, ET Bradley
University of Colorado and University of Central Florida

Cassini ISS, VIMS, UVIS spectroscopy and occultations show bright haloes around the strongest density waves. . We observe opposing effects: both small and large particles are found at the perturbed locations. Based on a predator-prey model for ring dynamics, we offer the following explanation: Cyclic velocity changes cause perturbed regions to reach higher collision speeds at some orbital phases, which preferentially removes small regolith particles; This forms a halo around the ILR; Surrounding particles diffuse back too slowly to erase the effect; Meteoritic bombardment creates fresh ice fragments at the regions of decreased regolith. Our explanation is based on the idea that moon-triggered clumping occurs at perturbed regions in Saturn's rings. Cyclic phase-plane trajectories forced around the stable point create both high velocity dispersion and large aggregates at these distances. Collisions between larger aggregates can cause compaction and merging, leading to gravity-bound aggregates that are even larger, and pump larger relative velocity. This explanation supports the view of a triple architecture of ring particles: a broad size distribution of particles; that aggregate into temporary rubble piles; coated by a regolith of dust. The aggregate model can explain many dynamic aspects of the rings; and the aggregates can also renew rings by shielding and recycling fresh ice.

Particle & Particle-Cluster Sizes in Saturn's Rings from Cassini Radio Occultations

Essam Marouf¹, Kwok Wong¹, Richard French², Nicole Rappaport³, & Colleen McGhee²
¹San Jose State University, ²Wellesley College, ³Formerly JPL/Caltech

Information about particle sizes in Saturn's rings is provided by differential extinction of three coherent sinusoidal radio signals transmitted by Cassini through the rings back to Earth (wavelength = 0.94, 3.6, and 13 cm,

respectively). The measurements are particularly sensitive to radii in the range $\sim 0.1 \text{ mm} < a < \sim 1 \text{ m}$. Complementary information is provided by measurements of collective near-forward scattering by the particles. The latter is captured in spectrograms of the received signals. Contributions of ring features of width as small several hundred kilometers can be identified and isolated in the measured spectra for a small subset of Cassini orbits of favorable geometry. Spectrograms measurements are sensitive to particles in the radius range $\sim 1 \text{ m} < a < \sim 20 \text{ m}$ and to spatially correlated aggregates of such particles (gravitational wakes). We use both inverse scattering and modeling techniques to recover the particle size distribution of 57 sub-regions of Saturn's C-Ring and few sub-regions of the Cassini Division. Power-law models of maximum particle radius $a_{\text{max}} \sim 5$ to 6 m, and power-law index $3.15 \leq q \leq 3.35$ characterize the Ring C background structure, with some subtle variations in the wavy region. Larger $a_{\text{max}} \sim 9$ m and smaller $q \sim 3.15$ characterize the outer ramp region. Surprisingly, even larger sizes $a_{\text{max}} \sim 25$ m appear to populate 4 of the Ring C "plateaus," possibly in aggregates form rather than as individual particles. In sharp contrast, particles of comparatively smaller maximum size appear to populate a fifth plateau region. In almost all C-Ring regions, the minimum radius a_{min} consistently falls in the few millimeters range. In ring regions where gravitational wakes are known to be present, such as the A and B Rings, the measured spectrograms show evidence for a strong forward scattering component consistent with scattering by spatially correlated and canted 'cylindrical' structures. We constrain the aggregate sizes, their canting angle, and other physical properties using comparisons of the observations with predictions of Monte-Carlo simulations of near-forward scattering by randomly blocked diffraction screen ring models. Example results are presented.

Searching for Clumps in Main Ring Spiral Density Waves

Rehnberg, M.E., Esposito, L.W., Sremcevic, M., Albers, N.

We report on the results of approximately 150 stellar occultations by the A and B rings of Saturn as observed by the High Speed Photometer of the Cassini Ultraviolet Imaging Spectrograph between 19 May 2005 and 2 July 2013. Previous examination of these stars as occulted by the F ring revealed a series of 56 statistically-significant features, many of which have been interpreted as clumps within the ring. We extend the search for these features to the A and B rings. In particular, we search the powerful Mimas 5:3 and Janus 5:4 spiral density waves for evidence of clumping action. A visual search has yielded a number of interesting features, but the amplitudes of periodic spiral density waves has resulted in difficulty interpreting these features as clumps similar to those observed in the F ring.

Propellers in Saturn's rings

M. Sremcevic, G. R. Stewart, N. Albers and L.W. Esposito
LASP, University of Colorado at Boulder, (Miodrag.Sremcevic@lasp.colorado.edu)

Propellers are the gravitational signature of bodies, or moonlets, embedded within the rings. Due to the three-body interaction of Saturn, moonlet, and ring particle, the orbital flow of ring particles is deflected creating characteristic "S" shaped structures.

In this paper we analyze two Cassini UVIS occultations of Bleriot, the largest propeller in Saturn's A ring. Comparing the occultation geometries to the observed detections in Cassini imaging data we show that the Bleriot propeller consists of an inner partial gap flanked by higher density wakes. Size and shape of the wakes are consistent with an embedded moonlet of about 400m in size. While in the UVIS occultations the partial gap is more prominent than the flanking wakes, the features seen in most of the Bleriot images are actually flanking wakes.

One of the most interesting aspects of the A ring propellers is their wanderings, or longitudinal deviations from a purely circular orbit. We numerically investigated the possibility of simple moon-driven libration. We found that some of A ring propellers indeed respond to the presence of Saturnian satellites. For instance, Earhart and Sikorsky are strongly perturbed by the mean longitude resonances with Pan.

In the B ring we discovered 12 propellers in 21 ISS NAC images (both lit and unlit geometry) and an additional signature in the UVIS beta Centauri Rev96 occultation. One of the detections is observed at two different epochs indicating a lifetime of at least 1.5 years.

Orbit evolution of disk-embedded masses: Directly observed in Saturn's rings

Matthew S. Tiscareno and Allegra E. Moran, Cornell University

Disk-embedded masses are thought to exist and evolve in many astrophysical contexts, including protoplanetary and protosatellite disks, stellar debris disks, and galaxies. The only known “ground truth” for these theorized objects is found in Saturn's rings.

The “propeller” moons within Saturn's rings are the first objects ever to have their orbits tracked while embedded in a disk, rather than moving through empty space (Tiscareno et al. 2010, ApJL). The embedded masses are not seen directly; rather, their locations are inferred by means of the propeller-shaped disturbances they create in the surrounding ring material (Tiscareno et al. 2006, Nature). Their observed orbits are primarily Keplerian, but with clear excursions in longitude on the order of $\pm 0.15^\circ$ longitude for the largest and best-studied example, and \pm several degrees longitude for others. Most theories that have been proposed to explain the non-Keplerian motion of propeller moons rely on gravitational and/or collisional interactions between the moon and the surrounding disk, and thus hold out the prospect for directly observing processes that are important in other astrophysical disk systems. The different models make different predictions, and future data will likely distinguish among them.

As part of its ongoing Solstice Mission, the Cassini spacecraft has intensified its campaign to characterize propeller orbits, and the more frequent sampling allows us to observe orbital change with improved temporal resolution. We will report the latest results of that observing campaign.

Microstructure and Composition

Comparison of Cassini UVIS Reflectance Spectra of Saturn's Rings to Compositional Models

Authors: ET Bradley, JE Colwell, LW Esposito

Far ultraviolet reflectance spectra of the rings are compared to Shkuratov and Hapke models to investigate the composition, mixing properties, and morphological properties of the rings. The ring particle albedo and ring particle phase function are determined at 5 nm intervals across the water ice absorption edge at 165 nm for the A, B, C rings and Cassini Division. Candidate non-icy materials with known optical constants in the far ultraviolet are used in the models to compare with the data. We find that a model with a discrete grain mixture where the water ice and contaminant grains have their own discrete sizes fit the data best suggesting that at short wavelengths the water ice grains and contaminant grains are distinguishable. Differences in the results between the Shkuratov and Hapke models suggest that photometric modeling of the rings should account for the fact that the rings are not a flat surface covered by regolith. We account for this using the retrieved ring particle phase function and find water ice and contaminant grain diameters less than 10 microns and porosities less than 0.5.

Study of Saturn's rings based on analysis of dust impact signals captured by Cassini RPWS

S.-Y. Ye¹, D. A. Gurnett¹, W. S. Kurth¹, T. F. Averkamp¹, S. Kempf², H.-W. Hsu², R. Srama^{3,4}, E. Grün², M. Morooka², S. Sakai⁵, J.-E. Wahlund⁶

¹Department of Physics and Astronomy, The University of Iowa, Iowa City, IA, USA

²Laboratory of Atmospheric and Space Physics, University of Colorado at Boulder, CO, USA

³IRS, University Stuttgart, Stuttgart, Germany

⁴Baylor University, Waco, TX, USA

⁵Department of CosmoSciences, Hokkaido University, Sapporo, Japan

⁶Swedish Institute of Space Physics, Uppsala, Sweden

The Cassini Radio and Plasma Wave Science (RPWS) instrument can detect dust particles when voltage pulses induced by dust impacts are observed in the wideband receiver. The size of the voltage pulse is proportional to the mass of the impacting dust particle. The dust impact signals measured by the dipole and monopole electric antennas are compared, from which the effective impact area of the spacecraft is estimated to be 4 m². In the monopole mode, the polarity of the dust impact signal is determined by the spacecraft potential and the location of the impact, which can be used to statistically infer the charge state of the spacecraft. RPWS measurements of dust particles from Saturn's E-ring and Enceladus show that the differential number density of dust particles can be characterized as a power law $dn/dr \propto r^\mu$, where $\mu \sim -4$ and r is the particle size, contradicting the narrow size distribution found by previous studies. The RPWS cumulative dust density is compared with the Cosmic Dust Analyzer (CDA) High Rate Detector (HRD) measurement. The differences between the two instruments are within the range of uncertainty estimated for RPWS measurement. The RPWS on-board dust recorder and counter data are used to map the dust density and spacecraft charging state within Saturn's magnetosphere. A new phenomenon called dust ringing has been found to reveal the electron density inside the Enceladus plume. The ringing frequencies, interpreted as the local plasma frequencies, are consistent with the values measured by other methods, i.e. Langmuir probe and upper hybrid resonance.

Observing Saturn's Rings in the Microwave with Cassini

Zhimeng Zhang

We will present calibrated, high 2.0×10^3 km)- and low 8.0×10^3 km)-resolution maps of Saturn's rings at 2.2-cm wavelength acquired by the Cassini radar radiometer. Microwave emission is the ideal waveband for studying the scattering properties of cm-scale ring particles and for constraining the thermal emission from (possibly buried) rocky ring contaminants, which, unlike water ice, behave like blackbodies at cm- wavelengths. While occultation observations are necessarily restricted to near-forward scattered light, scattered emission from Saturn (an extended source) can be viewed at a wide range of geometries. In order to successfully remove energy contributed by the radar's extensive side-lobes, we use an iterative self-calibration process. The current calibration reaches an RMS residual of 0.18 K (about 2% ring brightness temperature). The observed microwave brightness temperature of Saturn's rings is dominated by scattered Saturn emission and intrinsic thermal emission from the ring disk. We adopted a Monte Carlo multiple scattering model for the A, B and C rings that treats non-icy materials as inclusions in icy particles. Our results predict that the non-icy component of the C ring, assuming that contaminants emit with the dielectric properties of acidic rock, reach a maximum volume fraction of ~7% at the center of C ring and decreases toward its edges. These implications of these results for the origin and evolution the Saturn's rings will be discussed.

Thursday, August 14

Microstructure and Composition—Continued

Constraining the micro and macro-structure of the Saturn’s rings by modeling optical and thermal opposition phase curves of Cassini

Estelle Déau(a,b), Linda J. Spilker(a), Alberto Flandes(c), Ryuji Morishima(a), and the CIRS Ring Team

(a) NASA Jet Propulsion Laboratory, Pasadena CA, United States

(b) SETI Institute, Mountain View CA, United States

(c) Ciencias Espaciales, Instituto de Geophisica, UNAM, Mexico D.F., Mexico

The opposition effect is a strong increase of the brightness when the phase angle decreases to zero degree. So far, the rings’ opposition effect is observed in reflected and emitted light. The nature of rings’ optical and thermal opposition effect is still a matter of debate. Indeed, the most common theoretical hypothesis is that both effects are mainly caused by the shadow hiding, although the optical part should be partially due to the coherent backscatter. The bulk of the debate lies in the predominant, partial or null contribution of the coherent backscatter in the optical opposition effect. To study the opposition effect in reflected and emitted lights, we use imaging data from Cassini ISS, and thermal data of CIRS. To fully parameterize these data, we use an improved version of Bobrov’s logarithmic model. Comparisons between optical and infrared brightness opposition effect show that both surge amplitudes behave differently with the optical depth, therefore strongly suggesting distinct origin of the solar and thermal opposition effect. To probe the effect of the microscopic and macroscopic ring properties, we use UVIS optical depth and VIMS band depths profiles, and found strong correlations with the surge amplitude of respectively CIRS and ISS. As a result, our study favors the hypothesis that the optical opposition effect is due to regolith properties, and should be predominantly managed by the coherent backscatter.

Incomplete cooling of Saturn’s A ring at equinox: Implication for seasonal thermal inertia and internal structure of ring particles

Ryuji Morishima, Linda Spilker, Shawn Brooks, Scott Edgington (JPL), Estelle Deau, Stu Piorz (SETI)

The Composite Infrared Spectrometer (CIRS) onboard Cassini showed the lowest temperatures of Saturn’s rings ever observed at solar equinox in August 2009. The equinox temperature of Saturn’s A ring is found to be much higher than the model prediction regardless of ring structure assumed as long as the flux from Saturn is only taken into account. This temperature anomaly is likely to indicate incomplete cooling of ring particles at equinox, and this allows us to estimate the ring particle size and seasonal thermal inertia. We first assume that the internal density and the thermal inertia of a ring particle are uniform in depth. The particle size is estimated to be about 1 m. The seasonal thermal inertia is found to be as high as 50 in MKS units in the middle A ring whereas it is as low as 10 in MKS units or the diurnal thermal inertia in the inner A ring and outermost A ring. An additional model, where a particle has a high density core and thermal inertia gradient in the regolith layer, showed that the size of core radius is about 80 % of the particle radius for the middle A ring. The mean density of a ring particle with such structure is roughly half of the water ice density, consistent with that suggested from photometric azimuthal brightness asymmetry.

Measuring sub-centimeter particles in Saturn's A ring with Cassini UVIS stellar occultations

Tracy M. Becker¹, Joshua E. Colwell¹, Larry W. Esposito²

¹University of Central Florida

²LASP, University of Colorado, Boulder

The Ultraviolet Imaging Spectrograph (UVIS) on Cassini has detected diffraction spikes at the sharp edges that define the Encke Gap, the Keeler Gap, and the outer edge of Saturn's A ring in ~50% of the stellar occultations observed to date. The diffraction spikes are detected as photon counts near the ring edges that exceed the direct stellar signal by a few percent. The excess signal is due to forward-scattered light by populations of small (sub-centimeter) particles near the ring edges. The particle size distribution affects the magnitude and radial extent of the diffraction spike. We model the diffraction signal observed in each stellar occultation in order to place a limit on the size of the smallest particles and to constrain the slope of a power-law size distribution that describes the population of particles near each ring edge. We find a decrease in the radii of the smallest particles and a steepening of the power-law size distribution in the outer parts of the A ring, consistent with more energetic interparticle collisions due to satellite perturbations in that region. Additionally, the size distribution for a given edge fluctuates between occultations, suggesting a temporal or longitudinal variation along the ring edges.

Stellar Occultation Measurements of Particles in Saturn's Rings

Rebecca Harbison and Philip Nicholson

Occultations of rings have proven to be a useful way to measure the particle-size distribution of the bodies making up the ring. During stellar occultations of Saturn's rings observed by Cassini, we have observed 'gap overshoots' or 'horns': places near a sharp edge of the rings, such as the gaps of A Ring, where the transmission of starlight appears to exceed unity. This excess light is due to starlight forward-scattered from the nearby ring into the detector. In this work, we model these 'horns' in terms of a truncated power law particle-size distribution.

Due to the geometry of the observations and the observation wavelength of 2.92 microns, chosen to minimize reflected ringshine, our observations are sensitive to the distribution of ring particles from the millimeter to decimeter range. We model this using a truncated power law size distribution. We are able to model power law indices and minimum particle sizes and provide measurements or constraints within the C Ring and Cassini Division, and in the outer A Ring. Our models indicate that centimeter and millimeter-sized particles play a strong role in diffraction in the C and outer A Rings, with both a minimum particle size in the millimeter range, and a power law index of greater than 3 differential, but larger particles dominate the Cassini Division and its shallower power law index.

Small Particle Population in Saturn's Rings from Self-Gravity Wake Observations

Richard G. Jerousek¹, Joshua E. Colwell¹, Philip D. Nicholson², Matthew M. Hedman³, Larry W. Esposito⁴, Rebecca Harbison², and Robert A. West⁵

1. Department of Physics and Florida Space Institute, University of Central Florida, Orlando FL 32816, physics.cos.ucf.edu, 2. Department of Astronomy, Cornell University, Ithaca NY 14853 3. Department of Physics, Univ. of Idaho, Moscow ID 83844, 4. Laboratory for Atmospheric and Space Physics, Univ. of Colorado, Boulder CO 80309, 5. JPL, California Institute of Technology, Pasadena CA 91109

Saturn's rings consist of icy particles with sizes roughly following a power-law size distribution. Comparing optical depth measurements at different wavelengths is one way to measure this size distribution. This technique is complicated by the presence of self-gravity wakes. These aggregates are deformed by Keplerian shear leaving them with a characteristic cant angle of $\sim 25^\circ$ with respect to the direction of orbital motion resulting in geometry-dependent optical depth measurements. Thus, measurements made at different geometries and different wavelengths have combined effects of the self-gravity wakes and the particle size distribution. Here we present a method of extracting information about the size distribution of the particles in the gaps between the self-gravity wakes. The Cassini Visual and Infrared Mapping Spectrometer (VIMS) occultations measure starlight at an effective wavelength of $2.9 \mu\text{m}$ falling onto a single pixel of angular dimensions $0.25 \text{ mrad} \times 0.5 \text{ mrad}$ while Cassini Ultraviolet Imaging Spectrograph (UVIS) occultations measure starlight at a much smaller effective wavelength of $0.15 \mu\text{m}$ and over a field of view with larger angular dimensions of $6.0 \text{ mrad} \times 6.4 \text{ mrad}$. Starlight diffracted out of the VIMS pixel by particles smaller than $1.22\lambda_{\text{VIMS}}/2\theta \sim 8.86 \text{ mm}$, is not replaced by neighboring particles, while the UVIS instrument, with its larger field of view and smaller observed wavelength, collects all of the light diffracted by particles larger than $1.22\lambda_{\text{VIMS}}/2\theta \sim 0.025 \text{ mm}$. Consequently, measurements by the VIMS instrument overstate the optical depth by $\sim 1\text{-}2\%$ in regions where sub-centimeter-sized particles are present. Using the rectangular cross section (granola bar) wake model of Colwell et al. (2006, 2007) with a new free parameter to represent the VIMS optical depth, we combine VIMS and UVIS occultations for the first time. We find a significant fraction of sub-cm particles in the innermost and outermost portions of the A ring, in the B1 region of the B ring, and in several regions within the Cassini Division. In the Trans-Encke region, we find a trend of increasing abundance of sub-cm particles as the outer edge of the A Ring is approached, consistent with previous differential optical depth studies at radio wavelengths (Zebker et al. 1985) and greater erosion of weakly bound particle aggregates due to interparticle collisions where satellite perturbations are strong.

Dynamics and Kinematics

Deciphering the Embedded Wave in Saturn's Maxwell Ringlet

Richard G. French¹, Matt Hedman², Philip Nicholson³, Joseph Hahn⁴, Colleen McGhee-French¹, Joshua Colwell⁵, Essam Marouf⁶, Heikki Salo⁷, and Nicole Rappaport⁸

1: Wellesley College, 2: University of Idaho, 3: Cornell University, 4: Space Science, 5: University of Central Florida, 6: San Jose State University, 7: University of Oulu, 8: Jet Propulsion Laboratory

Saturn's Maxwell ringlet is a signature example of a sharp-edged freely-precessing ring with a substantial eccentricity, varying in width from about 20 to 100 km at a mean radius of about 87510 km. Embedded within the ringlet is a prominent wavelike structure with the appearance of an inward-propagating density wave (outer Lindblad resonance – OLR), but strongly modulated by the compression and expansion of the ringlet from periapse to apoapse. This wavelike structure, visible in Cassini ISS images (Porco et al. *Science*, 307, 1226), is observed at highest resolution in Cassini stellar (VIMS/UVIS) and radio (RSS) occultations, which reveal strongly non-linear structure in the wave crests and troughs at sub-km scales. Under the assumptions (justified a posteriori) that the radially integrated optical depth of the ringlet is independent of ring longitude relative to periapse and that the unperturbed mean optical depth profile varies with longitude in a linear, accordion-like manner, we have determined the principal characteristics of the embedded wave. Using wavelet decomposition to estimate pairwise differences in phase of the wavelike structure, we have identified the wave as an $m=-2$ OLR with a pattern speed $\Omega_p = 1769.16 \text{ deg day}^{-1}$ and a resonance radius of 87532.8 km, towards the outer edge of the Maxwell ringlet. This is very close to the f-mode $l=2$ $m=2$ OLR associated with a Saturn internal oscillation, predicted to lie at 87400 km in the Maxwell gap by Marley and Porco (*Icarus*, 1993, vol. 106, p. 508, Table IV). We determine the wave phase across the ring from fits to periodic wave structure, and then develop a simple linear density wave model that nicely matches the overall behavior of the waves over eight years of observations and for all true anomalies. This simple model fails, however, to reproduce the detailed extreme nonlinear structure of the waves. We employ the Hahn and Spitale (*Ap. J.* 2013, 772:122) symplectic N-body integrator to construct more realistic models of the Maxwell ringlet, based on a streamline approach to calculate the effects of self-gravity. The code successfully reproduces the principle characteristics of the nonlinear behavior of the wave, which exhibits clear variations in structure from

periapse to apoapse, in response to the compression and expansion of the ring. From both wavelet analysis and numerical simulations, we estimate an average surface mass density of about 15-20 gm cm⁻². The mass of the fictitious satellite driving the wave is about $3 \times 10^{-11} M_{\text{Saturn}}$. A fundamental limitation of the current implementation of the self-gravity streamline model is that streamlines do not cross, and in the actual Maxwell ringlet, it is likely that close particle interactions are important, especially near periapse under conditions of high particle density. We will report on more realistic N-body simulations of the effects of ringlet compression and expansion on three-dimensional wave structure, compared to the observations.

Collisions between Gravitational Aggregates in the Tidal Field

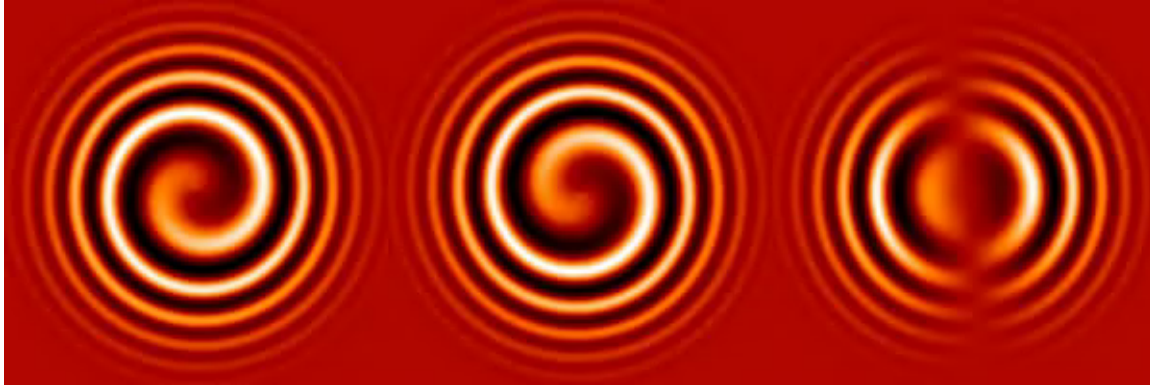
Authors: Ryuki Hyodo, Keiji Ohtsuki, Kobe University

Outcomes of collisions in free space are determined by specific impact energy, and the mass fraction of the largest remnant is a monotonically decreasing function of impact energy. However, it has not been shown whether such a relationship is applicable to collisions under the influence of a planet's tidal force, which is important in ring dynamics and satellite accretion. In the present work, we examine the collisional disruption of gravitational aggregates in the tidal environment by using local N-body simulations. We find that outcomes of such a collision largely depend on the impact velocity, the direction of impact, and the radial distance from the planet. In the case of a strong tidal field corresponding to Saturn's F ring, collisions in the azimuthal direction are much more destructive than those in the radial direction. Numerical results of collisions sensitively depend on the impact velocity, and a complete disruption of aggregates can occur even in impacts with velocity much lower than their escape velocity. In such low-velocity collisions, the deformation of colliding aggregates plays an essential role in determining collision outcomes, because the physical size of the aggregate is comparable to its Hill radius. On the other hand, the dependence of collision outcomes on impact velocity becomes similar to the case in free space when the distance from the planet is sufficiently large.

A Prominent m=1 Standing Wave in the Cassini Division

Colleen McGhee-French¹, Richard G. French¹, Philip Nicholson², Matt Hedman³, Joshua Colwell⁴, Essam Marouf⁵, and Nicole Rappaport⁶ 1: Wellesley College, 2: Cornell University, 3: University of Idaho, 4: University of Central Florida, 5: San Jose State University, 6: Jet Propulsion Laboratory

The outer Cassini Division, between the Laplace gap's outer edge (OEG) near 120090 km and the inner edge of the Bessel gap (IEG) at 120240 km, is host to a ramped structure with very conspicuous wavelike structure. This 150 km wide region features a prominent peak in normal optical depth ($\tau \sim 0.5$) near 120000 km, gradually decreasing to $\tau \sim 0.1$, with large amplitude oscillations about 10 km in wavelength. As part of a program to determine the accurate orbits of ringlets, gaps, and ring edges in Saturn's rings from the full set of Cassini radio (RSS) and stellar (UVIS/VIMS) occultations, we have determined that this pattern is an m=1 standing wave, W120.1, with about 9 visible wave crests varying in wavelength between 5 and 20 km, decreasing outwards, with a fixed pattern speed of 4.72 deg day⁻¹ and an approximate resonance location of 120075 km. The pattern speed is nearly identical to that of the Laplace OER and OEG, consistent with the suggestion that the wave is driven by the Laplace ringlet. As shown in the figure below, the fixed wave pattern originates from coaddition of the outward-propagating wave (left) and its inward-propagating reflection upon reaching the Bessel IEG (middle), resulting in the standing wave at right.



A wavelet analysis of the structure reveals an anticorrelation between normal optical depth and surface density, with a surface density of about 0.2 gm cm^{-2} in the inner, higher optical depth region, rising to 0.4 gm cm^{-2} in the outer, lower optical depth region.

Kronoseismology II: Further searches for Saturn-driven waves in the C ring.

Phil Nicholson (Cornell U.) and Matt Hedman (U. Idaho)

In previous work we identified 6 inward-propagating density waves in the C ring as driven by outer Lindblad resonances (OLRs) with internal f-mode oscillations in Saturn (Nicholson & Hedman [2013], *Astron. J.* 146, 12). The oscillations involved are sectoral modes (ie., $l = m$) with $m = 2, 3$ and 4 . We have now examined additional C ring waves from the catalog of Baillie et al. (2011), in an attempt to identify weaker and/or shorter-wavelength waves. We use the same wavelet technique to measure the phase difference between pairs of waves, and compare this to the predicted value for specified values of 'm' and the assumed pattern speed. Our results include the following: (1) Two new f-modes, one with $m = 10$ (W83.63 = Rosen-h) and the other with $m = 5$ or 11 (W81.02 = B14); (2) Confirmation of the Mimas 6:2 and Pandora 4:2 density waves identified by Baillie et al.; (3) Identification of 5 outward-propagating waves between radii of 84,800 and 86,600 km as $m = 3$ density waves with pattern speeds between 807 and 834 deg/day, spanning the reported range of Saturn rotation periods. The simplest interpretation is that these are driven by 3:2 tesseral resonances with gravitational anomalies fixed within the planet.

Waves requiring further study include an $m = 1$ OLR-type wave (W85.67 = Rosen-d) within plateau P6 (Hedman & Nicholson, 2014 DDA), and a prominent wave within the Maxwell ringlet (see R.G. French et al., this meeting).

Particle clustering in periodically forced planetary rings.

S.J. Robbins^{1,*}, G.R. Stewart¹, L.W. Esposito¹. ¹LASP, 3665 Discovery Dr., University of Colorado, Boulder, CO 80309. *stuart.robbins@colorado.edu

Cassini UVIS data show variable clumping on the edges of Saturn's rings, including the outer edges of the A and B rings, where they are strongly perturbed by satellites. A model to explain the perturbation was proposed in [1] for a classic "predator-prey" scenario where there is interplay between mass aggregations and mean velocity, but it remains to be seen whether dynamical N -body simulations show the same effect. We are working to quantify how resonant forcing modifies both the degree of particle clustering and the ring viscosity on orbital timescales.

This work was based on the REBOUND N -body code under open-source licensing [2]. We used the shearing boundary conditions and symplectic epicycle integrator (SEI) modules. Every $1/40^{\text{th}}$ of an orbit, the position and velocity vector of every particle, and a screenshot were saved. Additionally, the viscosity of the cell was calculated per the method of [3].

Our forcing method only simulates radial forcing, neglecting the azimuthal variation of the satellite's gravitational potential and approximating the radial variation with a periodic function. Our implementation of the forcing function is to add another acceleration term to the SEI:

$$q \sin(\delta \cdot t.d) \sin(2\pi x / L_x),$$

where q is the magnitude of the forcing, δ is a "detuning" parameter such that the forcing is not at the natural resonance, $t.d$ is the decimal portion of the orbit ($0 \leq t.d < 1$), and L_x is the radial size of the cell.

We will present our results-in-progress showing the effect of this forcing on the rings' properties, which demonstrate behavior similar to simulations of the perturbed edge of the Encke Gap [4].

References:

- [1] Esposito et al. (2012) doi:10.1016/j.icarus.2011.09.029.
- [2] Rein & Liu (2012) doi:10.1051/0004-6361/201118085.
- [3] Daisaka et al. (2001) doi: 10.1006/icar.2001.6716.
- [4] Lewis & Stewart (2005) doi:10.1016/j.icarus.2005.04.009.

On the Origin of Eccentric Narrow Rings

Glen R. Stewart, LASP, Univ. of Colorado, Boulder, CO

The origin of the eccentric shape of many narrow rings in the Saturn and Uranian ring systems has so far lacked a satisfactory explanation. For modes that grow on time scales much longer than the orbit period and for azimuthal length scales that are of the order of the circumference of the ring, the orbital dynamics is well-approximated by the slow guiding center motion. This reduced description is described by Hamilton's equations, where the mean longitude measured in a rotating reference frame, $y = (\lambda - \Omega t)r_0$, is the only coordinate, and the canonical momentum, $p = (\kappa^2/2\Omega)(a - r_0)$, is proportional to the difference of the semimajor axis, a , from a reference radius, r_0 , which is conveniently set equal to the mean radius of the narrow ring.

The kinetic equation for a self-gravitating ring resembles the kinetic equation for one-dimensional plasmas,

$$\frac{\partial f}{\partial t} - 4 \left(\frac{A\Omega}{\kappa^2} \right) p \frac{\partial f}{\partial y} - \frac{\partial \Phi}{\partial y} \frac{\partial f}{\partial p} + \frac{\partial \Phi}{\partial p} \frac{\partial f}{\partial y} = 0$$

where A is the Oort constant.

The Greens function that relates the distribution of ring particles to the gravitational potential is a modified Bessel function once the equation has been Fourier-transformed with respect to the mean longitude,

$$\Phi_m(p) = -2GM_{part} \int dp_1 K_0 \left(\frac{2\Omega m}{\kappa^2 r_0} |p - p_1| \right) f_m(p_1)$$

where m is the Fourier transform variable, and M_{part} is the mass of a ring particle.

Whereas the shape of the velocity distribution plays a central role in the plasma problem, it is the radial surface density profile, $f_0(p)$, that plays the analogous role for narrow rings. Inviscid self-gravitating rings have growing eccentric modes if the radial density profile exhibits a local minimum. A flat-topped radial profile where the second derivative is zero is the marginally stable case.

Gravitational Accretion of Particles onto Moonlets Embedded in Saturn's Rings

Yuki Yasui (Kobe Univ.), Keiji Ohtsuki (Kobe Univ.), and Hiroshi Daisaka (Hitotsubashi Univ.)

Using local N-body simulation, we examine gravitational accretion of ring particles onto moonlets in Saturn's rings. We find that gravitational accretion of ring particles onto moonlets is unlikely to occur at radial locations interior to the outer edge of the C ring, unless the density of the moonlets is much larger than that of water ice or non-gravitational cohesive forces play a major role. Detailed analysis of accretion process of individual particles onto moonlets shows that particle accretion onto high-latitude regions of the moonlet surface occurs even if the rings' vertical thickness is much smaller than the moonlet's radius. The degree of particle accretion in outer rings is found to depend significantly on rings' vertical thickness and optical depth. Our results suggest that large boulders recently inferred from observations of transparent holes in the C ring are likely to be collisional shards, while propeller moonlets in the A ring would be gravitational aggregates formed by particle accretion.

Friday, August 15

F Ring

The Stable F Ring Core: Antiresonance plus Corotation Resonance

Jeff Cuzzi, Essam Marouf, Dick French, Bob Jacobson

The stability of the narrow F Ring core in a sea of orbital chaos may be due to an unusual “antiresonance” at a series of specific locations in the F Ring region, where apse precession between synodic encounters with Prometheus allows subsequent semimajor axis perturbations to promptly cancel before significant orbital period changes can occur. This cancellation, however, fails for particles that encounter Prometheus near their periapse when Prometheus is near its apoapse; the strength of the semimajor axis perturbation is then highly nonsinusoidal in encounter longitude and difficult to cancel on a subsequent encounter. Only particles that consistently encounter Prometheus *away* from these antialigned longitudes can maintain stable orbits, implying that the true mean motion n_F of the stable core must be defined by a corotational resonance of the form $n_F = n_p - k_p/m$, where (n_p, k_p) are Prometheus’ mean motion and epicycle frequency. The prediction is that the “massive” F Ring core material, only sporadically detected by RSS, is actually confined to a series of short longitudinal clumps separated by nearly empty longitudes. Small particles spread quickly in azimuth and obscure this clumpy structure. To test this prediction, we have used a set of 24 Cassini RSS (and VGR) detections and 43 nondetections. We determine the inertial longitudes of the detections and nondetections for a comb of candidate n_p , precess them to a common epoch and fold them modulo the anticipated m -number of the resonance (Prometheus $m=110$ OCR), to see if clustering appears. Results will be shown and discussed.

Gravitational and Collisional Processes at Saturn’s F Ring

C.D. Murray, N.J. Cooper, N.O. Attree, G.A. Williams, M.W. Evans

Submitted by Evans

The unusual and dynamic nature of the narrow F ring of Saturn, which exhibits a variety of features changeable over timescales from hours to years, can be understood by considering the combined effects of gravitational and collisional interactions with local objects. Such objects range in size from the large satellites Prometheus and Pandora down to small ~ 1 km moonlets either embedded in the ring or on nearby orbits.

Gravitational perturbations from the two ‘shepherding’ satellites produce the regular ‘streamer-channel’ features as well as triggering the formation of clumps. ‘Fans’ are created gravitationally by smaller moonlets embedded in the ring itself. ‘Jets’ and ‘mini-jets’ are respectively large- and small-scale features created by collisions of a local population of moonlets with the core of the F ring. The mini-jets are caused by low velocity collisions while the jets are due to higher velocity encounters with more distant objects probably representing the upper end of the moonlet population in size and orbit.

We will present the latest results derived from *Cassini* data, primarily from reprojected radius-longitude mosaics of the ring, and we look forward to the observations to be made in the final year of the mission.

Comparison of Clumps in Saturn's F Ring from Voyager and Cassini

Robert S. French, Shannon K. Hicks, Mark R. Showalter, Adrienne K. Antonsen, Douglas R. Packard; SETI Institute, 189 Bernardo Ave., Mountain View, CA 94043; rfrench@seti.org

Among the phenomena observed in Saturn's F ring are diffuse extended bright clumps (ECs) $\sim 3\text{--}40^\circ$ in longitudinal extent. These ECs appear, evolve, and disappear over a span of days to months. Showalter (2004, *Icarus*, 171, 356–371) analyzed all Voyager images of the F ring and found that there were 2–3 major and 20–40 minor ECs present in the ring at any given time. We expand upon these results by comparing the ECs seen by Voyager to those seen by Cassini in 2004–2010. We find that the number of minor ECs has stayed roughly constant and the ECs have similar distributions of angular width, absolute brightness, and semimajor axis. However, the ECs are now much dimmer relative to the mean ring background and the common exceptionally bright ECs seen by Voyager are now exceedingly rare, with only two instances seen by Cassini during the six years.

For there is nothing covered, that shall not be revealed: Unveiling Saturn's F ring at ring plane crossing

Britt R. Scharringhausen

On 1-2 December 2005, the Cassini spacecraft passed through Saturn's ring plane, traveling from the dark side of the rings to the sunlit side. In the four hours before the ring-plane crossing (RPX), the brightness of the rings, as measured in VIMS images, doubled. A model of the ring system indicates that as the main-ring opening angle decreased to zero, the far side of the F ring was revealed. However, the observed brightening is significantly later than would be predicted by the geometry of the main rings and the F-ring orbits of Bosh et al. (2002) or Albers et al. (2012). Although the longitude of the ascending node is less well-determined than the F ring's other orbital parameters, the observed timing cannot be reproduced by varying it. The localized F-ring clumps present during this observation are not sufficient to account for the pre-RPX brightening. We explore other potential solutions of varying physical plausibility.

Origin, evolution

Recent results on Chariklo's rings

Maryame El Moutamid (Cornell University), Matt Hedman (Idaho University), Bruno Sicardy (LESIA/UPMC Paris Observatory), Matt Tiscareno (Cornell University), Daniel Tamayo (Cornell University), Phil Nicholson (Cornell University), Joe Burns (Cornell University).

On June 3, 2013, a multi-chord stellar occultation revealed the unexpected presence of two dense rings around 10199 Chariklo, the largest Centaur object with a radius of 124 ± 9 km. The two rings have respective orbital radii, widths and normal optical depths of $a_1 = 391$ km, $W_1 = 7$ km, $\tau_1 = 0.4$ and $a_2 = 405$ km, $W_2 = 3$ km, $\tau_2 = 0.06$. They are separated by a clear gap about 9 km wide (Braga-Ribas et al. 2014).

The presence of those rings has been confirmed during several other stellar occultations observed over the past few months (February and April 2014).

This is the first ring system ever observed around a small solid body. The existence of such a system raises several questions as to the origin and evolution of rings around such an object. The small number of minor planets surveyed thus far suggests that Chariklo's rings may not be an isolated case.

We will present additional results on azimuthal variations in the rings, estimate the masses of their putative shepherding satellites, and suggest possible models for the rings' formation.

Evolution of Structure and Composition in Saturn's Rings Due to Ballistic Transport of Micrometeoroid Impact Ejecta.

P. R. Estrada (CSC, SETI Institute), R. H. Durisen (U. of Indiana), and J. N. Cuzzi (NASA Ames)

We introduce improved numerical techniques for simulating the structural and compositional evolution of planetary rings due to micrometeoroid bombardment and subsequent ballistic transport of impact ejecta. Our current, robust code, which is based on the structural code of Durisen et al. (1989, Icarus 80) and the pollution transport code of Cuzzi and Estrada (1998, Icarus 132), is capable of modeling structural and bulk compositional changes over long times on both local and global scales. We provide demonstrative simulations to compare with previous work, as well as examples of how ballistic transport can maintain observed structure. Our preliminary results imply that one very key piece missing from our efforts that is likely critical for maintaining observed features such as the C ring plateaus is the inclusion of a retrograde-biased ejecta component. Such a component would come about if impacts were destructive rather than merely cratering. We are currently integrating this into our model. We acknowledge the recent Cassini observation (Kempf et al. 2013, AGU) that suggests that the micrometeoroid flux at Saturn may be considerably lower than previously thought, and predominantly of different dynamical origin. We will address the implications of these observations for the ballistic transport process in Saturn's rings.

Dynamics of Uranus' dusty μ ring

Hsiang-Wen Hsu, Mihály Horányi, Sascha Kempf
LASP, University of Colorado Boulder, CO, USA

The dynamics of small (micron and submicron sized) dust particles in planetary rings are of particular interest because, in addition to gravity, they are also sensitive to various other forces, and thus are able to illustrate subtle processes that cannot be probed otherwise. Studying the processes that shape planetary rings comprised of small particles provides important constraints on their sources / sinks, transport processes, as well as clues on the history and evolution of these rings. Here we present preliminary results about the dynamical simulations of Uranus' dusty rings. Our simulations suggest that micron-sized particles in the recently discovered μ ring need to be positively charged to remain confined in the observed region (planet-centric distance of 86,000 to 103,000 km). The ultimate goal of this study is to provide a comprehensive theoretical understanding of the dust environment around Uranus in preparation for in situ dust measurements and dust hazard assessments for future missions.

Satellite Formation from Circumplanetary Particle Disks

Ryuki Hyodo¹, Keiji Ohtsuki¹, Takaaki Takeda²
¹Kobe University, ²VASA Entmt. Co. Ltd

Most planets in the Solar system have satellite systems. Single satellite systems such as the Earth-Moon system have a relatively massive satellite compared to the host planet's mass. On the other hand, giant planets such as Jupiter,

Saturn, and Uranus have multiple-satellite systems. Generally, their inner major satellites called regular satellites exist outside their Roche limit with relatively small mass ratio to the host planet. Those inner satellites are on nearly circular prograde orbits with low inclinations. We examine the formation processes of satellites as a consequence of viscous spreading of circumplanetary particle disks initially confined within planet's Roche limit by using N-body simulations. We find that a relatively massive satellite is formed just outside Roche limit from relatively massive disks. With decreasing initial disk mass, formed satellites become smaller and migrate outward by a large distance. We will examine orbital evolution of formed satellites in detail, and also discuss dependence of the mass of formed satellites on the initial disk mass.

Accretion of the Moon from the protolunar disk

Julien Salmon, Robin M. Canup

The most favored scenario for the origin of the Earth's Moon involves a collision between a large impactor and the Earth toward the end of its formation, putting material into orbit and forming a disk around the Earth, from which the Moon accreted. In the "canonical" case, the impactor is a Mars-sized object and forms a disk composed primarily of material from the impactor, which could be at odds with the identical isotopic composition of the Earth and Moon. In the "non-canonical" scenario, involving either a collision between two objects of similar size, or a high-velocity impact on a rapidly-rotating Earth, the disk and post-impact Earth have very similar compositions. But in these cases, the Earth-Moon system's angular momentum is too large by a factor ~ 2 , and subsequent capture of the Moon into the evection resonance with the Sun is required to drain this excess of angular momentum. We have developed a hybrid numerical model to study the accretion of the Moon from the protolunar disk, accounting for some important thermodynamical effects in the disk, in particular the limitation of the disk's viscosity by its ability to radiate its energy. While pure N-body models predicted accretion timescales of ~ 1 year, we find that the Moon assembles in 3 consecutive steps over ~ 200 years, and forms significantly farther than previously estimated. We will discuss what these new accretion dynamics imply for the different impact scenarios.

What happens to the Keeler gap when Daphnis decides to move out?

Radwan Tajeddine, Matthew S. Tiscareno, Matthew M. Hedman, Phil D. Nicholson, Joseph A. Burns

Abstract: Jacobson (2014, DDA) recently reported that Daphnis changed its orbital motion by the equivalent of a 3 km increase in its semi-major axis at some time between 2010 and 2012. Since this moon is responsible for holding open the Keeler gap, such a change in the satellite's orbit should show effects on the gap's edges. We will present preliminary results, from the Cassini ISS images, of the radial position of the outer edge and the wavelength in the gap edges formed by Daphnis' encounter with ring particles. The available data cover the period both before and after the orbit's change.

We will also mention other behaviours of the edges, such as the unexpectedly strong second-order Daphnis perturbation on the outer edge, and unexpectedly complex response of the inner edge to the $m=32$ resonance with Prometheus (Tiscareno et al. 2005, DPS).

Ring environment

Saturn's other Ring current

F. J. Crary (1)

(1) Laboratory for Atmospheric and Space Physics, University of Colorado, United States
(frank.crary@lasp.colorado.edu)

Saturn's main rings orbit the planet within an atmosphere and ionosphere of water, oxygen and hydrogen, produced by meteoritic impacts on and ultraviolet photodesorption of the ring particles [Johnson et al., 2006; Luhmann et al., 2006; Tseng et al., 2010]. The neutral atmosphere itself has only been tentatively detected through ultraviolet fluorescents of OH [Hall et al., 1996] while the ionosphere was observed in situ by the Cassini spacecraft shortly after orbital insertion [Coates et al., 2005; Tokar et al. 2005, Waite et al. 2005].

Although the plasma flow velocity of this ionosphere is not well-constrained, the close association with the rings suggests that its speed would be coupled to the keplerian velocity of the rings themselves. As a result, the motion of the plasma through Saturn's magnetic field would produce an induced voltage, oriented away from the planet outside synchronous orbit and towards the planet inside synchronous orbit. Such a potential could result in currents flowing across the ring plane and closing along magnetic field lines and through Saturn's ionosphere at latitudes between 36° and 48°. Cassini observations of whistler-mode plasma wave emissions [Xin et al., 2006] centered on synchronous orbit (1.76 Rs, mapping to 41° latitude) have been interpreted as a product of field-aligned electron beams associated with such a current.

This presentation will investigate the magnitude of these currents, the resulting torques on the ring ionosphere and rings, and the consequences for the ring ionosphere.

References

- Coates, A.J., McAndrews, H.J., Rymer, A.M., Young, D.T., Crary, F.J., Maurice, S., Johnson, R.E., 2005. Plasma electrons above Saturn's main rings: CAPS observations. *Geophys. Res. Lett.* 32, L14S09.
- Johnson, R.E., Luhmann, J.G., Tokar, R.L., Bouhram, M., Berthelier, J.J., Sittler, E.C., Cooper, J.F., Hill, T.W., Crary, F.J., Young, D.T., 2006. Production, ionization and redistribution of Saturn's O₂ ring atmosphere. *Icarus* 180, 393–402.
- Luhmann, J.G., Johnson, R.E., Tokar, R.L., Ledvina, S.A., Cravens, T.E., 2006. A model of the ionosphere of Saturn's rings and its implications. *Icarus* 181, 465–474.
- Tokar, R.L., and 12 colleagues, 2005. Cassini observations of the thermal plasma in the vicinity of Saturn's main ring and the F and G rings. *Geophys. Res. Lett.* 32, L14S04.
- Tseng, W.-L., W.-H. Ip, R.E. Johnson, T.A. Cassidy, M.K. Elrod, 2010. The structure and time variability of the ring atmosphere and ionosphere. *Icarus* 206, 382–389.
- Waite Jr., J.H., and 10 colleagues, 2005. Oxygen ions observed near Saturn's A ring. *Science* 307, 1260–1262.
- Xin, L., D. A. Gurnett, O. Santolik, W. S. Kurth, and G. B. Hospodarsky, 2006. Whistler-mode auroral hiss emissions observed near Saturn's B ring. *J. Geophys. Res.* 111, A06214, doi:10.1029/2005JA011432

OPUS: Now with Enhanced Geometric Metadata for Cassini Optical Remote Sensing Instruments

Mitchell K. Gordon, Mark R. Showalter, Lisa Ballard, Neil Heather
Carl Sagan Center, SETI Institute, Mountain View, CA

The PDS Rings Node has developed and incorporated into our search tool, the Outer Planets Unified Search (OPUS), detailed geometric metadata about Saturn and its rings and satellites. OPUS now supports with enhanced metadata Cassini ISS, VIMS, and UVIS data sets. CIRS data sets will be supported later this year.

This extensive set of geometric metadata is unique to the Rings Node and enables search constraints such as latitudes and longitudes (Saturn, Titan, icy satellites, and rings), viewing and illumination geometry (phase, incidence and emission angles), ring open angles (to observer and to the sun), and distances and resolution. Unique parameters include the effective ring radial resolution - the radial resolution in km/pixel as projected onto the ring plane. This distinction is important because the rings can be highly foreshortened, in which case the actual resolution in the ring plane is much coarser than the standard resolution would indicate. We also provide metadata to support an additional coordinate frame used to describe the geometry of nearly edge-on views of the rings. The data base also includes identification of all rings and bodies in the field of view of each observation, not just the intended target.

OPUS also supports (without enhanced geometric metadata) data sets obtained by Cassini CIRS (data obtained through June 2010), New Horizons LORRI (Jupiter), Galileo SSI, Voyager ISS and IRIS, and Hubble (ACS, WFC3 and WFPC2). We will be adding Cassini and Voyager ring occultations in the near future.

We are preparing to release a completely revamped user interface, OPUS2. It is faster and enables even more powerful search capabilities. Let us know if you are interested in helping us Beta test OPUS2.

OPUS: <http://pds-rings.seti.org/search/>

The mass flux of micrometeoroids into the Saturnian system

S. Kempf (1,2), N. Altobelli (3), M. Horányi (1,2) and R. Srama (4)

(1) LASP, University of Colorado at Boulder, Boulder, United States (sascha.kempf@lasp.colorado.edu),

(2) IMPACT, NASA SSERVI, United States, (3) ESA, ESAC, Spain, (4) IRS, Stuttgart University, Stuttgart, Germany

There is an ongoing debate about the age of Saturn's rings being: a) rather young, or b) formed contemporaneously with the planet and its satellites. The water ice rings contain about 5% of rocky material, originating from the continuous bombardment of the rings by interplanetary micrometeoroids. Knowledge of the incoming mass flux would allow to estimate the ring's exposure time. Model calculations suggest exposure times of 108 years, implying a late ring formation. This scenario is problematic because, for example, the tidal disruption of a Mimas-sized moon or of a comet within the planet's Roche zone would lead to a much larger rock content than observed today.

Here we report on the first direct measurement of the meteoroid flux into the Saturnian system by Cassini's Cosmic Dust Analyzer (CDA). We measured the impact velocity vectors of about 140 extrinsic micrometeoroids with radii $\geq 2 \mu\text{m}$, and determined their orbital elements. On the basis of these measurements we determined the mass flux into the Saturnian system. Our findings suggest a ring exposure time of 4.5 billion years and is in support of an early ring formation scenario.

Reception

Tuesday, August 12

5:30-7:30pm

Millennium Hotel – 1345 28th Street

Please join us at a reception Tuesday evening, in the back courtyard of the Millennium Hotel. There will be light snacks and a cash bar. This is free for all attendees. See map in Getting Around section.

Dinner

Pre-registration required

Wednesday, Aug. 13

6:30pm

Cantina Loredo – 1680 29th Street, in the 29th Street Mall

Please bring your ticket(s) to the dinner. They are in your badge holder.

Pre-registered guests will meet at Cantina Loredo for a plated, sit-down workshop dinner. You will choose from the menu when at your table. If you didn't pre-register any dietary restrictions, please tell the Cantina as soon as you get there.

The restaurant is about a 15 minutes walking distance of Millennium Hotel or LASP.

See map in Getting Around section.

Getting Around

AROUND LASP



LASP consists of two buildings: LASP Space Technology Building (LSTB) and the Space Science building (SPSC).

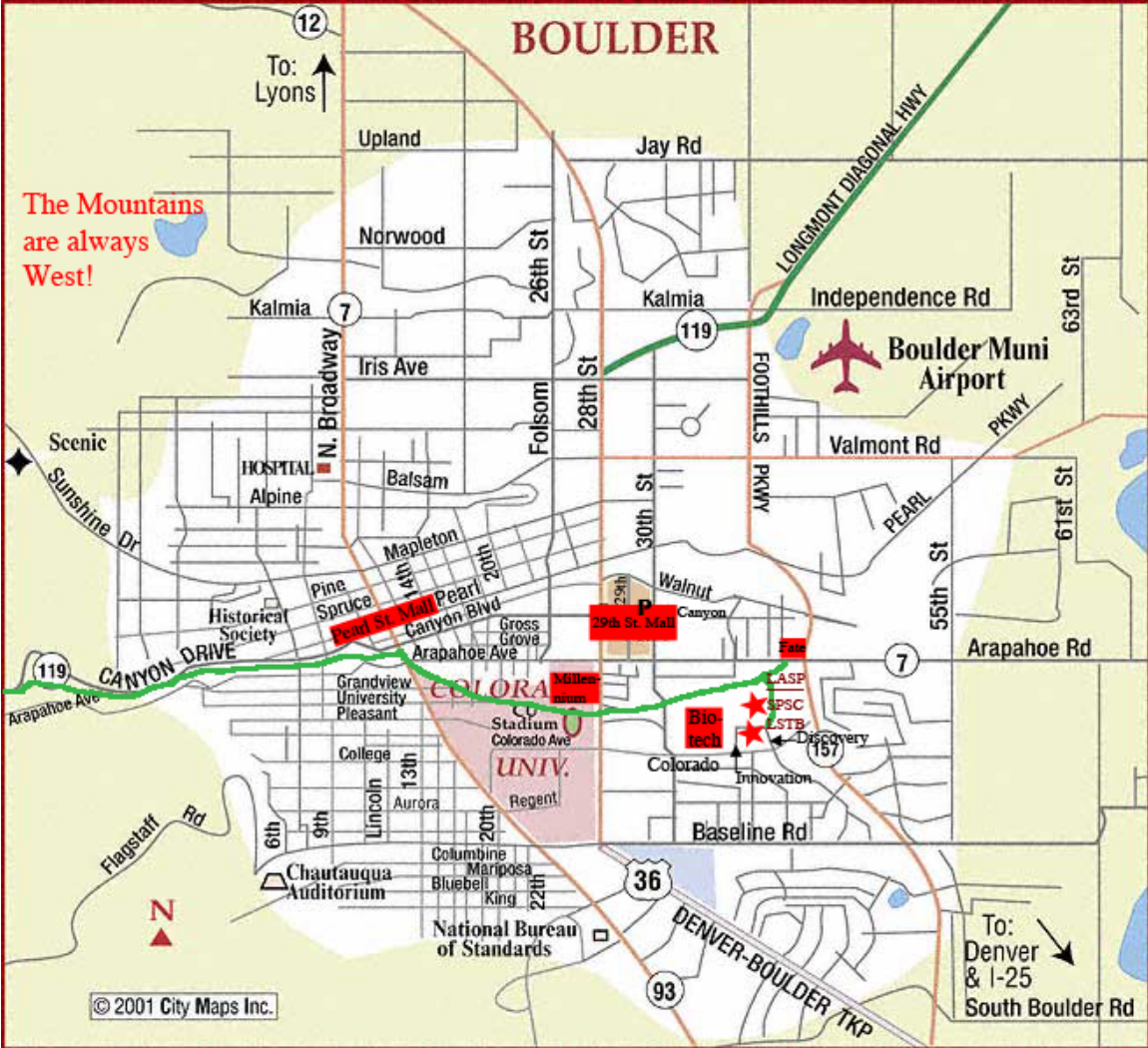
WALKABLE (also see larger map on back):

Etai's (Udi's) Cafe - In the Biotech building, 2nd floor, front/south side. Go up the outside steps and turn left. ~5-8min.

Fate Brewery - Take bike path on the east side of SPSC and go north behind the building (then veer right at the fork onto the Boulder Creek Path) to Arapahoe Ave. Fate is on the opposite side of Arapahoe. You can cross at the light to the west ~10-15min.

29th Street Mall (lots of restaurants) - Take the Boulder Creek Path. Get there by walking through the parking lot behind the Biotech building and taking a right/north at the end of the drive at the married student apartments (past the playing fields). Go left/west on the Creek Path. You can either 1) go up on top of the overpass and go right/north on 30th, go left on Arapahoe, then right (cross the street) into the 29th St. Mall. Or, 2) go down under the overpass, walk past Scott Carpenter Park and take the path on the far side of the park right/north toward Arapahoe, cross over Arapahoe into the 29th St. Mall. ~25-30 min depending on location.

Millennium Hotel - Take Boulder Creek path to back side of hotel; ~25min. (See 29th Street Mall directions for how to get to path.) Or walk to 30th, then west on Arapahoe to 28th Street; ~30 minutes.



29th Street Mall Restaurants

The 29th Street Mall has many restaurants, most fast-casual. Parking in the surface lots can be nearly impossible during lunchtime, so just go into the parking garage off of Canyon and walk to your destination (bring this map).

From LASP into parking garage: West (toward mountains) on Colorado. North (R) on 30th. West (L) on Canyon. First right into the parking garage.

* Laura's favorites

| | | | |
|-----------------------------------|----|--------------------------------|----|
| BJ's Restaurant and Brewery | 1A | Motomaki (sushi) – coming soon | 1A |
| California Pizza Kitchen | 1C | Native Food Café (vegan) | 1A |
| Cantina Laredo (Mexican) | 1B | Noodles & Company | 1A |
| Chipotle (Mexican fast food) | 1A | Panera Bread | 1C |
| Daphne's California Greek | 1A | Peet's Coffee & Tea | 1A |
| Fireouse Subs | 1A | Pei wei Asian Diner | 1A |
| Five Guys Burgers and Fries | 1C | Protien Bar (healthy) | 1C |
| Garbanzo Mediterranean Grill * | 1C | Smashburger | 1A |
| Jamba Juice | 1A | Spooners Frozen Yogurt | 1C |
| Mad Greens (salads) | 1C | Starbucks | 1D |
| modMarket (salads, pizza, soup) * | 1A | | |



There are also some great restaurants in the strip mall on the north side of Arapahoe west of 29th St. Mall between 28th St. and Folsom Ave. Pizzeria da Lupo*, CubaCuba*, Zolos, Rincon Argentino*, Larkburger, Bistro Tasuki* (sushi)-on the west side of Folsom, and others as well.